Risk stratification for stent fracture prediction in percutaneous pulmonary valve implantation through patient-specific finite element analysis

Cosentino D[1], Pennati G[2], Capelli C[3], Diaz-Zuccarini V[1], Bonhoeffer P[3], Taylor AM[3] and Schievano S[3]

1- UCL, Department of Mechanical Engineering, London, UK

2- Politecnico di Milano, LaBS, Laboratory of Biological Structures, Milano, Italy

3- UCL, Institute of Cardiovascular Science, London, UK

This research is funded by the European Union 7th Framework Programme (FP7/2007-2013) under grant agreement n° 238113 (project MeDDiCA).

Introduction

The device currently in use for percutaneous pulmonary valve implantation (PPVI) (Melody™, Medtronic Inc, Minneapolis, MN, USA) has already been successfully implanted in over 3,000 patients worldwide, but a major technical issue still remains: stent fracture [Lurz, 2009]. The main reasons for fracture have not yet been identified, and preliminary experimental and computational analyses were not able to predict this problem observed in 25% of the treated patients [Nordmeyer, 2007; Vezmar, 2010; Schievano, 2010], suggesting that the stent in-vivo loading conditions were incorrectly reproduced. Thus, a novel methodological patient-specific approach was developed for enhancing the modelling of PPVI stent *in situ* configurations and its loading conditions. The aim of this study was to carry out risk stratification for PPVI stent fracture by analysing the asymmetries of the stent *in vivo* shape and by performing patient-specific finite element (FE) analyses.

Material and Methods

Forty-two PPVI patients were chosen for this study according to the following inclusion criteria: (i) PPVI procedure carried out in a catheterisation laboratory equipped with Axiom Artis Flat Detector (Siemens, Germany) to eliminate image distortion [Vano, 2005]; (ii) fluoroscopy exams performed with 2 orthogonal projections (antero-posterior and lateral); and (iii) device visible in the fluoroscopy images throughout the balloon expansion procedure and at least during one cardiac cycle after implantation. The patients' population included 10 patients (24%) who experienced fracture in the first 6 months after the implantation and 32 patients (76%) in which no fracture occurred in the same timeframe. Informed consent for research use was given by the patients or by their parents in case of minor age.

Three dimensional (3D) *in situ* device geometries were reconstructed for every patient at 3 different times of the procedure and cardiac cycle, post-processing the orthogonal biplane fluoroscopy images [Schievano, 2010]. Calibration of the fluoroscopy images was achieved by identifying the straightest strut of the stent in both projections. As geometrical dimensions of the stent are known, the images were scaled in order to equal the length of the chosen strut to its real length of 5.78 mm. Additionally, in 16 patients it was possible to calibrate the images also with the markers of a Mullins balloon (NuMed Inc, Hopkinton, NY, USA) used for PPVI stent post-dilatation. Differences in the scaling factors obtained with the strut-based and the marker-based calibration were considered negligible (<4.6%). The intersection points between the struts forming the stent were identified in both projections. Using computer aided design (CAD) commercial software (Rhinoceros, McNeel, USA), the selected points were projected into the 3D space by tracing parallel rays. By connecting the strut junctions through straight segments, the zigzag wires of the stent were reproduced in 3 dimensions, defining the whole *in situ* stent structure for each patient (fig.1 left). The superimposition of the 3 reconstructions from the procedure with the reconstruction of the stent while still crimped onto the balloon catheter (fig.1, centre and right) allowed us to measure the displacements of every junction point from its initial position to the pre-recoil state, through systole and diastole.

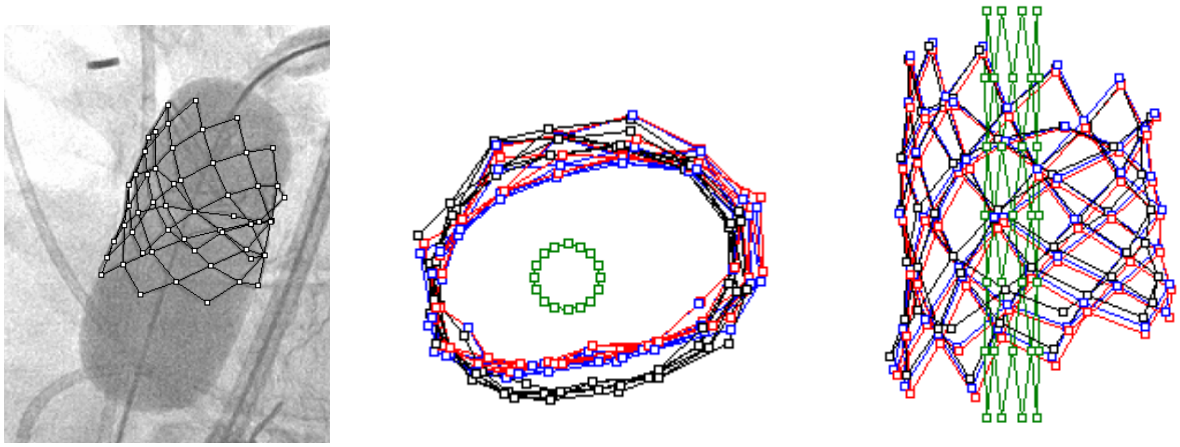

Figure 1 – (left) Stent 3D reconstruction from fluoroscopy image of the patient at the end of the balloon expansion; superimposition of the reconstructions done at the pre-recoil (black), systole (red) and diastole (blue) with the initial crimped stent shape (green) for one patient: top (centre) and lateral (right) views.

A FE model of the stent was created with the commercial CAD software Rhinoceros (McNeel, USA) resembling the device crimped onto the catheter, using data supplied from the company or obtained from measurements by means of caliper and optic microscopy. Golden coverings of the stent around the crown welds were included in the model. The presence of the biological valve was discarded, as it is unlikely to affect stent fracture. Following mesh sensitivity analysis, 792,640 hexahedral elements with reduced integration were used, including 60 elements on the cross-section of the stent wire (fig. 2).

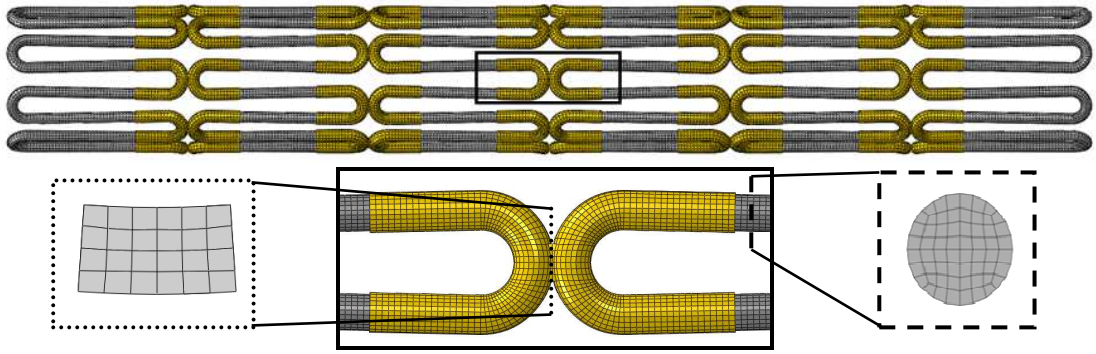

Figure 2 – FE model of the device in its crimped configuration without the biological valve inside; zoom to show the structured hexahedral mesh of the link between crowns (bottom left) and the wire sections (bottom right).

Finite element patient-specific stent deployment configurations were replicated in Abaqus/Standard (Simulia, USA) applying the displacements previously calculated to the stent nodes in correspondence of the strut junctions. Particularly, the displacements were applied at the central node of the wire central section in correspondence of the outer crowns, and on the central node of the rectangular central section of the links between the internal crowns. Five steps were simulated for each patient. First, the stent was led from its initial crimped status to the end of the inner balloon inflation of the balloon-in-balloon delivery system (10 mm of internal diameter); second, the further expansion of the stent was mimicked following the inflation of the outer balloon (pre-recoil); finally, the effect of systole and diastole were replicated starting from the end of balloon inflation. Results were analysed in terms of stress distribution, and by performing a fatigue analysis using both the Goodman and the Sines criteria.

A thorough analysis of stent geometry and geometry variations after balloon deflation at the end of the procedure and during the cardiac cycle was conducted in the two groups of patients, fractured and non-fractured. Together with other geometrical information at different levels of the stent (struts, cells, sections and whole structure), the asymmetries of the stent *in vivo* shape were calculated as follows [Schievano, 2010]:

a) 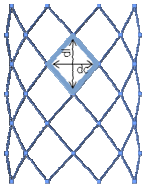 b) 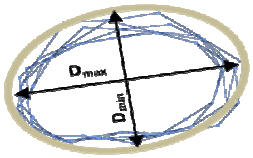

c) 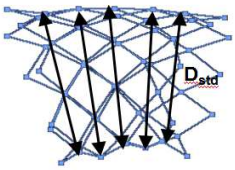

a) circumferential asymmetry C_a evaluated with the ratio between the cell longitudinal diagonal *dl* and the circumferential diagonal *dc*;
b) radial asymmetry R_a evaluated with the ratio between the maximum diameter *Dmax* and the minimum diameter *Dmin* at each section;
c) longitudinal asymmetry L_a evaluated through a standard diameter *Dstd* calculated at each section.
Results from the two groups were compared and risk stratification for stent fracture was obtained.

Results and Discussion

Radial asymmetry proved to be the most significant parameter for fracture prediction (fig. 2): stents with a more elliptical shape present higher risk of failure.

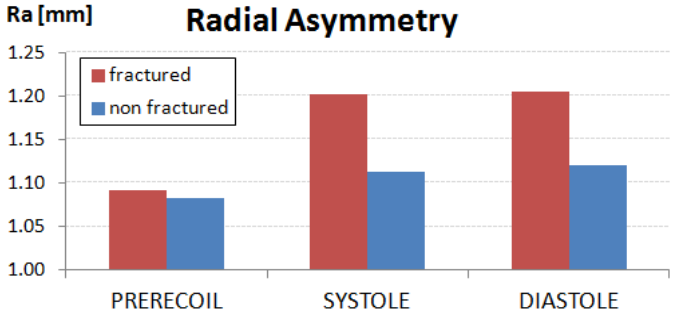

Figure 2 – Radial asymmetries values averaged for the fractured (red) and non fractured (blue) groups respectively at prerecoil (1.09±0.05 and 1.08±0.03), at systole (1.20±0.17 and 1.11±0.04), and at diastole (1.21±0.18 and 1.12±0.05) . The difference between the two groups was statistically significant (prerecoil: p-value=0.361; systole: p-value=0.018; diastole: p-value=0.044).

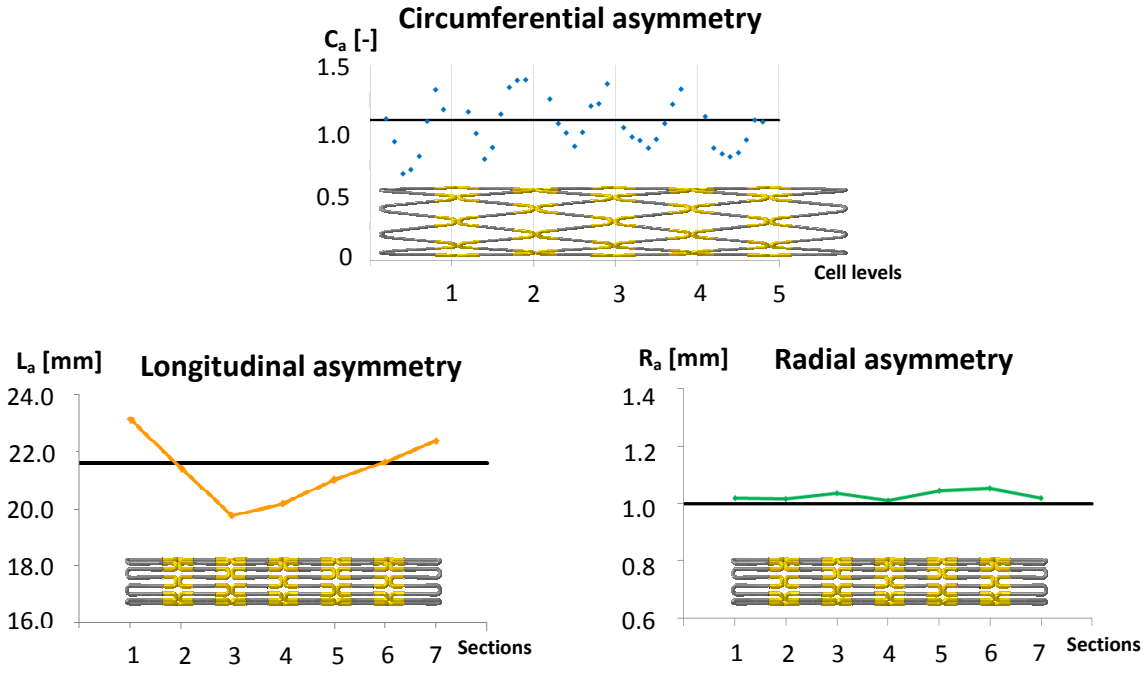

Figure 3 – Circumferential (blue), longitudinal (orange), and radial (green) asymmetries for one fractured patient at systole: results compared with the case of a stent symmetrically deployed at 22 mm (black).

However, it is a combination of multiple different asymmetries that leads to stent fracture: for example, in patients as the one shown in figure 3 with symmetrically expanded stent, both in the radial (1.05 mm, averaged on all sections) and circumferential directions (1.033 averaged on all cells), but with a high longitudinal asymmetry (22.06 mm, averaged on all sections), which means higher Von Mises stresses, fractures occurred. At the moment, further statistical analyses are being carried out, for a better evaluation of the risk stratification, taking into account additional parameters regarding the change in shape of the stent after the balloon deflation (recoil) and during cardiac-cycle. Patient-specific FE stent expansions in literature refer to stent models expanded inside patient-specific vessel anatomies (usually reconstructed from MR or CT images) by means of either a pressure load applied to the internal surface of the stent [Gijsen, 2008; Schievano, 2010], or including the model of a balloon to be pressurized inside the stent [Capelli 2012]. However, these approaches do not guarantee the achievement of a stent deformation identical to the patient's one, thus losing accuracy in the real loading conditions reproduction. On the contrary, with the FE nodal displacement approach proposed in this study, it was possible to obtain the exact stent deformed configurations as in the patient. In every case, the highest value of Von Mises stress occurred close to the openings at the strut intersection, which are the most highly bent portions of the device (fig. 4). In general, stent configurations with higher radial and longitudinal asymmetries across the studied population reported higher Von Mises stresses. The maximum Von Mises stress (633 MPa) was reached in the fractured group, where also the fatigue criteria confirmed a larger number of elements above the fracture limit. In the majority of the cases it was verified that the location of fractures, detected from X-rays images, was included in the areas at highest risk for fracture as predicted by the simulations.

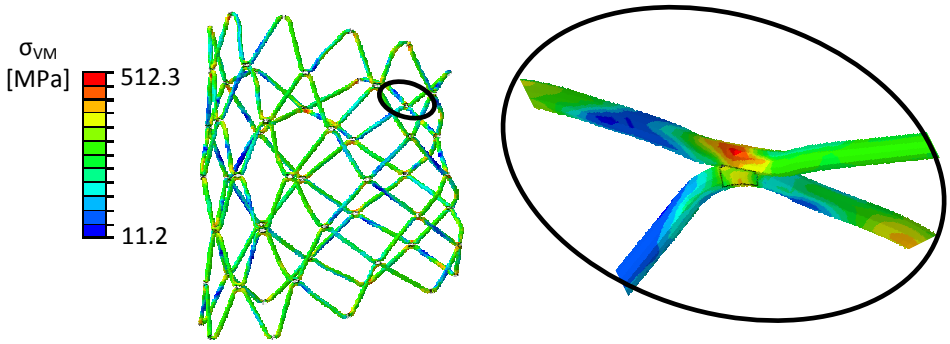

Figure 4 – Von Mises stress distribution in one patient-specific case. Zoom on the openings at the strut intersection where the highest values of stress were localised.

Conclusion

In this work a novel patient-specific FE stent expansion was used for the first time, proving that realistic loading conditions can provide accurate information regarding the stent mechanical performance and its fatigue life in each subject. Therefore, the results of patient-specific FE simulations could aid in planning a tailored follow-up for each patient, in order to monitor for possible stent fractures according to the risk predicted by the computational analysis. Furthermore, a better understanding of the physical phenomena inducing fracture in PPVI stents coupled with pre-PPVI implantation site anatomical and dynamic information could help predict success/failure of the procedure for each individual patient before the procedure is performed. Hence, patient selection for PPVI could be aided by engineering tools along with conventional clinical assessment towards safer implantation and more successful results.

References

Capelli *et al*, Medical and Biological Engineering and Computing, 50(2): 183-192, 2012.
Gijsen *et al*, BioMedical Engineering OnLine 7(23), 2008.
Lurz *et al*, Expert Review of Cardiovascular Therapy, 7(7):1-10, 2009.
Nordmeyer *et al*, Circulation, 11:1392-97, 2007.
Schievano *et al*, Journal of Biomechanics, 43(4):687-693, 2010.
Vano *et al*, Physics in Medicine and Biology, 50(23):5731-42, 2005.
Vezmar *et al*, Journal of American College of Cardiovascular Intervention, 3:439-48, 2010.